Photodissociation of Complex Nuclei at Energies between the Mesonic Threshold and 1150 Mev*

CHARLES E. ROOS†
Vanderbilt University, Nashville, Tennessee

AND

VINCENT Z. PETERSON
California Institute of Technology, Pasadena, California

(Received July 18, 1961)

The photodisintegration of complex nuclei by gamma rays up to 1150 Mev has been studied by exposing nuclear emulsion to bremsstrahlung from the CalTech electron synchrotron and observing the "photostars" produced. Exposures were made at 16 different peak energies between 250 and 1150 Mev. Nearly 10 000 photostars were analyzed for star frequency, prong number, angular distribution, and (at 1143 Mev) the visible energy release per star. The bremsstrahlung yield of multiprong (≥ 2 prong) stars increases abruptly as photons capable of producing pions are included. The cross section per photon, derived from the bremsstrahlung yield by the photon difference method, is essentially constant at 250 microbarns/nucleon at all energies above 300 Mev. A model for photostar production is given which involves photopion production followed by absorption or scattering of the pion and recoil nucleon. Experimental free-nucleon photopion cross sections are used, together with the Monte Carlo calculations of Metropolis *et al.*, to determine the probability for star formation. Good agreement with both the shape and magnitude of the excitation curve is obtained if nuclear motion is included. Mean and maximum prong numbers for photostars are the same as for stars produced by pions or protons of equal available energy. The mean-free-paths in nuclear matter of pions and protons are short, so that photostar yields are a measure of the integrated total photomeson cross section. More than 95% of the multiprong stars made by 1-Bev bremsstrahlung are made by photons whose energies exceed the pion production threshold of 150 Mev. Most of the 1-prong events are produced by photons below 150 Mev, and the yield is consistent with giant resonance (γ,p) reactions plus "pseudo-deuteron" photodisintegration, a process whose cross section rapidly decreases as the photon energy increases. Variation of mean prong number with energy and comparison with nuclear cascade calculations suggests that the excitation of the residual nucleus is nearly constant at 100 Mev over a wide range of incident photon energies. The visible energy release per photostar shows a linear dependence on prong number, and more than half of the photon energy is carried away by neutral particles.

I. INTRODUCTION

THE character of photonuclear reactions can be expected to vary with the wavelength of the incident photon. The λ of the "giant resonance" photons (10 to 20 Mev) is 20 to 10 fermis and the interaction cross section depends strongly on the dipole moment of the whole nucleus. In the energy range between the "giant resonance" and the mesonic threshold, nuclear subunits are of major importance. Since a *n-p* pair or "quasi-deuteron" has an electric dipole moment and λ for a 100-Mev photon is 2 fermis, it is reasonable that the "quasi-deuteron" model can explain most of the observed phenomena in this energy range. At the mesonic threshold (150 Mev) λ is comparable to the diameter of a free nucleon, and above 300 Mev the nucleus can be treated as an assembly of free nucleons. The transition regions are not precisely defined and the "quasi-deuteron" model is useful both for some phenomena of the "giant resonance" and at energies slightly in excess of the mesonic threshold. The bulk of the data discussed in the present paper will deal, however, with energies sufficiently in excess of the "quasi-deuteron" region that the independent nucleon model appears to be the most significant.

Each energy range has a characteristic type of event. The "giant resonance" photons interact with the dipole moment of the whole nucleus and the resulting nuclear emission can be described by a statistical or evaporation process. In view of the Coulomb barrier neutron emission is some 100 times more prevalent than proton ejection. The peak cross sections are on the order of 100 mb for the (γ,n) and $(\gamma,2n)$ processes. There has been extensive work at these energies, and reviews of the theory[1] and experimental data[2] are available.

In the energy range between the giant resonance and the mesonic threshold the "quasi-deuteron" model first proposed by Levinger[3] predicts that the primary photon interaction is between *n-p* pairs, often resulting in the ejection of *n-p* pairs from the target nucleus. Several observers have found both the predicted *n-p* correlation[4,5] and have also shown that the photoprotons are emitted with a strongly forward angular distribution with the predicted discontinuity in the energy spectra.[6] The investigations of neutron-proton coincidences resulting from the bombardment of lithium and helium with 220-Mev bremsstrahlung led Barton and Smith[7] to the conclusion that most of the fast photoprotons can be explained in terms of the quasi-deuteron model. Mesonic processes would not be expected to be important for 220-Mev bremsstrahlung.

* This work was supported in part by the U. S. Atomic Energy Commission, the Research Corporation, and the National Science Foundation.

† Experimental data obtained while at the University of California, Riverside, California, and the California Institute of Technology, Pasadena, California.

[1] J. S. Levinger, Ann. Rev. Nuclear Sci. **4**, 13 (1954).
[2] K. Strauch, Ann. Rev. Nuclear Sci. **2**, 105 (1952).
[3] J. S. Levinger, Phys. Rev. **84**, 43 (1951).
[4] M. Q. Barton and J. H. Smith, Phys. Rev. **95**, 573 (1954).
[5] A. C. Odian, P. C. Stein, A. Wattenberg, B. T. Feld, and R. Weinstein, Phys. Rev. **102**, 837 (1956).
[6] C. Levinthal and A. Silverman, Phys. Rev. **82**, 822 (1951).
[7] M. Q. Barton and J. H. Smith, Phys. Rev. **110**, 1143 (1958).

In the "mesonic" region (i.e., photon energies above 150 Mev) the primary interaction can be considered to be between the photon and a single nucleon, resulting in the production of one or more real mesons. The scattering of pions and recoil nucleons, and pion absorption within the target nucleus can then result in the formation of a star. Several observers have exposed nuclear emulsions to a direct bremsstrahlung beam and all have found that the number of events with two or more charged particles rises very sharply above the mesonic threshold.[8–11]

It is difficult to use the "quasi-deuteron" model to explain the sudden rise in photostar production above 150 Mev, since the real deuteron photodisintegration cross section is decreasing. Furthermore, the observed increase is in multiprong events, as distinct from single fast protons expected from deuteron photodisintegration. An "optical model" which includes the photoproduction of real pions from the individual nucleons, the pions being subsequently reabsorbed to give rise to a photostar, furnishes a natural explanation of the observed phenomena. We have already used this model in I (reference 11), and now extend it by taking into account nuclear motion, the formation of nuclear cascades by the recoil nucleon as well as the pion, and by inclusion of more recent data on photoproduction of pions from free nucleons.

In summary, photonucleon reactions can phenomenologically be roughly grouped into three energy ranges. The "giant resonance" processes account for most of the zero-prong (all neutral particle) stars, as well as some 1- and 2-prong stars. The quasi-deuteron process most often gives rise to one-prong events (proton-neutron pairs), while the mesonic effects most often give rise to multiprong stars.

This paper is an extension of our earlier work[11] on photostar production by 250- to 500-Mev bremsstrahlung. The photostar excitation curve was determined at a number of energies up to 1.15 Bev. About 10 000 single- and multiple-pronged events were analyzed and then compared with the total photomeson production cross section. This includes 3000 events from I.

"Photostars" are photodisintegration processes in emulsion which yield two or more charged particles. They may be produced by photons of any energy up to the maximum energy of the bremsstrahlung. In order to learn the properties of photostars produced by a given energy photon one must resort to the "photon difference method," a subtraction process of properly normalized exposures at adjacent bremsstrahlung energies. This method was discussed in I.

Nuclear emulsion is a mixture of light and heavy elements, and identification of the photodisintegrating nucleus for a particular event is rarely possible. However, several features of high-energy photodisintegration tend to minimize this ambiguity. First of all, high-energy photons have very short wavelengths and interact primarily with the individual nucleons. Secondly, the interaction mean-free-path in nuclear matter for high-energy gamma rays is sufficiently long so that all nucleons are equally affected. Thus we can consider the first stage of high-energy photodisintegration to affect the individual nucleon in both light and heavy nuclei approximately equally. The principal difference between light (C, N, O) and heavy (Ag, Br) nuclei is nuclear radius and, therefore, reabsorption probability.

II. EXPERIMENTAL PROCEDURE

Exposure

Single Ilford G-5 emulsions 400-μ thick were exposed at normal incidence to a collimated bremsstrahlung beam of the electron synchrotron of the California Institute of Technology. Exposures were made at a series of energies from 430 to 1143 Mev. These energies supplement the earlier exposures from 250 to 500 Mev reported in I. The bremsstrahlung beam was produced by electrons striking a 0.031-in. tantalum radiator; although this represents 0.20 radiation units it is known from pair spectrometer measurements[12] that a "thin-target" spectrum results when only the central portion of the beam is viewed. Our exposures were highly collimated in order to produce a well-defined area (approximately 3 cm^2) which was completely scanned. Typical exposures were between 2 to 7×10^7 Mev/cm^2, a range we judge optimum from consideration of statistics, signal/noise ratio, scanning efficiency, and beam monitoring. All of the beam striking the plate was monitored by a thick wall ion chamber calibrated[13] at several energies using the quantameter developed by Wilson.[14] The new calibrations of the ion chamber are in excellent agreement with the older values at 500 Mev used for the cross section in I. Typical values of the monitor sensitivity (at STP) in units of 10^{18} Mev/coulomb are 4.88 at 500 Mev, 5.55 at 800 Mev, and 5.85 at 1100 Mev.[13] The charge from the ion chamber is collected on a standard capacitor. Corrections of about 10% to the published cross sections used in I were found necessary due to the effects of ac pickup on the standardized capacitor. The ion chamber charge was characteristically of the order of 10^{-9} coulomb for the photostar exposures. Considerable care was taken to minimize drift and to standardize the capacitor. The beam saturation effects were measured and found to be negligible for the ion currents encountered in this experiment. The total estimated error in the integrated beam intensity is 4%. As noted in I, the peak energy of the bremsstrahl-

[8] R. D. Miller, Phys. Rev. **82**, 260 (1951).
[9] S. Kikuchi, Phys. Rev. **86**, 41 (1952).
[10] E. P. George, Proc. Phys. Soc. (London) **A69**, 110 (1956).
[11] V. Z. Peterson and C. E. Roos, Phys. Rev. **105**, 1620 (1957), hereafter referred to as "I".
[12] J. Boyden and R. L. Walker (unpublished).
[13] R. Gomez (private communication).
[14] R. R. Wilson, Nuclear Instr. **1**, 101 (1957).

ung is determined by a magnetic field integrator to less than 2%.

Scanning Procedure

We have defined a photostar as a nuclear event with two or more visible prongs greater than 5 μ, a minimum range to eliminate nuclear recoils and miscellaneous "blobs." The classification of events and the general scanning procedures were very similar to those discussed in I. In particular the correction for scatterings in the 2-prong events was shown to be negligible. In order to maintain accurate beam monitoring, we exposed relatively small areas on the emulsion and scanned the entire beam area. (Earlier experience with sampling techniques, using photometry to estimate the variation of beam intensity over the irradiated area, gave systematic errors associated with the difference between low-energy darkening of the plate and the high-energy photostar pattern.) Scanning efficiencies for all plates were determined by duplicate scanning; despite the apparent ease in detecting photostars, we have learned that systematic checking procedures are essential. Our lowest efficiency for $\geq$2-prong stars was 90%, and with duplicate scanning most of the missing events are of course found.

The high photostar cross section at higher energies considerably simplifies background problems. The total exposure is limited by the large slow-electron background from the low-energy region of the bremsstrahlung. Increasing the peak energy adds high-energy photons to the spectrum which produce photostars, but has negligible effect on the electron background within the emulsion. This permits a higher area density of photostars (300–700 stars/cm^2) than in I. The spurious stars from radiothorium were identified by their characteristic prong length and ionization (see I). Less than 10% of the stars in the exposed region were identified as this type. This number is consistent with the area density of thorium stars found in the unexposed regions and on control plates. The background for cosmic rays was measured with control scans and was subtracted from the photostar counts. It is approximately 1% of the total number of stars in the high-energy plates.

In addition to the measurement of star position and prong number the ionization of each prong was estimated. A rough measure of the angular distribution of both fast ("gray") and slow ("black") star prongs was obtained by measuring the forward/back ratio. Since the emulsions were exposed at normal incidence this ratio was obtained for some 2500 prongs by simply recording whether the prongs were directed towards the air surface or the glass backing. The tracks were classified as "black" if more than 70% opaque (approximately 80 Mev for protons), "gray" if less than 70% and more than 2$\times$ minimum grain density, and "light" if less than 2$\times$ minimum.

In this experiment the emulsion is the target as well as the detector. The weight and area of each pellicle was determined prior to exposure. The emulsion thickness for plates was determined by selecting a sample plate from each emulsion batch. Variations of about 2% in emulsion thickness from plate to plate were recorded.

Scanning for 1-Prong Events

The production of single tracks was found to be quite copious at all beam energies. Sample areas were separately scanned. Considerable care was necessary to accurately locate each 1-prong event, and to achieve unambiguous identification. The range, projected angle, and opacity were recorded to identify all single tracks greater than 5 μ in length. With these precautions the average one-prong detection efficiency was 85%. This efficiency was measured by a triple scan of the entire sample areas of the 1150-Mev plate and overlapping portions of the lower energy plates.

The background of stars not due to the bremsstrahlung exposure was determined by examining unexposed regions of the emulsion adjacent to the beam. This would include *n-p* recoils, cosmic-ray events and one-prong thorium stars. This correction was approximately 10% of the 1-prong events in the exposed region.

Both glass-backed plates and pellicles were used for the 1-prong star scan. The plates permitted a direct comparison with the lower energy plates (250 Mev) used in I. The pellicles and plates were compared and the number of spurious one-prong events from the glass backing of the plates was found to be less than 10%.

Detailed analysis of 100 photostars at 1150 Mev.—A stack of 20, 4 in.$\times$6 in., 400-μ G-5 emulsions (see Table I) was lightly exposed (3×10^5 Mev/cm^2) with the emulsion plane parallel to the beam. Since the exposure had to be very light to minimize the electron background from showers, the pre-exposure cosmic-ray background was relatively much more important. For this reason only stars of 2 or more prongs of which at least 1 prong could be traced to adjoining pellicles were accepted. The range, angle, and gap density of all prongs from the "traceable" stars were measured. Most of the prongs stopped within the stack. The type of prong (alpha, pion, proton) could be determined, but it was not feasible to separate protons from deuterons in this exposure. The energy distribution, energy release, and angular distribution were determined.

III. EXPERIMENTAL RESULTS

Integral Yields

The integral yield over the bremsstrahlung spectrum, or "cross section per equivalent quantum," $\sigma_Q = N/Qnt$, is given in Table I for various peak bremsstrahlung energies E. N is the number of stars, and nt the number of nucleons per cm^2 in emulsion thickness. The yield is normalized per emulsion *nucleon* in order to facilitate comparison with the theoretical model; in order to express σ_Q per emulsion *nucleus* (excluding hydrogen) multiply the values given in Table I by 49.6 (the

TABLE I. Normalized yields σ_Q of photostars for various prong number stars at various peak bremsstrahlung energies (E). σ_Q is the yield per equivalent quantum. $Q=W/E$, where W = total bremsstrahlung energy. Yields given here are per *nucleon*; multiply by 49.6 to obtain yields per *emulsion nucleus* (excluding hydrogen). The total bremsstrahlung flux (in Q) and emulsion thickness (t) are also given.

E	Exposure ($Q\times10^{17}$)	Prong number 1	2	3	4	5	6	7	8	9	≥10	≥2 prongs	≥3 prongs	F/B ratios Gray and Black	light
251[a]	9.64		30±3	18±2	7.9±1	1.9±0.4	0.4±0.2	0.1			0.1	59±10	29±2		
275[b]	6.80	520±80	29±5	23±3	9.2±2	5.5±2	1.7±0.8	0.4				69±6	40±3		
294[a]	8.50		33±6	28+2	15 ±2	3.8±0.8	1.4±0.6	0.4				78±10	46±3		
376[b]	3.55		46±11	47±7	22 ±4	9.8±3	3.3±2					128±12	82±8		
425[b]	3.38	460±50	62±8	39±6	38 ±6	13 ±3	9.0±3	3.3±2				164±12	102±8		
430[e]	3.46		76±5	54±4	34 ±3	20 ±3	8.8±2	1.2±0.4	0.6			196±10	120±7	1.3	2.5
452[b]	2.44		77±20	50±8	32 ±6	16 ±4	10 ±4	1.0±0.8	1.0	1.0		188±15	111±15		
475[b,c]	4.52		90±14	54±6	42 ±5	17 ±3	6.8±2	1.8±1	0.4	0.4	0.7	213±10	123±12		
495[d]	1.92	405±80	76±8	57±6	38 ±5	18 ±3	7.4±2	2.6±1	1.0	1.1		201±12	125±9	1.3	2.5
503[b,c]	4.85		86±8	57±6	43 ±5	28 ±4	12 ±3	3.6±2	2.3±1			232±8	145±12		
665[e]	2.30	470±55	106±9	84±8	47 ±5	33 ±4	15 ±2	7.5±2	3.1±1	1.8	1.3	297±14	192±11		
726[d]	2.53		90±8	69±6	48 ±5	35 ±5	15 ±3	9.4±2	3.7±1	2.0±1	0.4	274±14	184±11		
880[d]	0.77	570±80	112±14	72±10	61 ±9	46 ±8	20 ±5	8.1±3	8.1±3	5.4±3	1.3	333±21	220±14	1.3	1.8
910[e]	1.17		109±12	82±9	62 ±9	36 ±6	22 ±4	12 ±3	2.8±2	2.8±2	2.8±2	330±19	221±14	1.2	1.8
1120[e]	5.24	605±70	104±8	95±8	61 ±7	43 ±5	27 ±4	16 ±3	7.5±2	5.2±2	6.7±4	365±15	262±11		
1143[e]	0.98		102±14	99±10	76 ±10	42 ±7	28 ±5	14 ±4	16 ±4	7.4±3	5.3±3	389±23	287±20	1.3	2.4

[a] G-5 plates; $t=0.1570$ g/cm^2. [b] G-5 plates; $t=0.0684$. [c] G-5 plates; $t=0.0758$. [d] K-5 pellicles; $t=0.1667$ to 0.1721. [e] G-5 plates; $t=0.1665$.

TABLE II. The constituents of the target emulsions (Ilford G-5).

Element	g/cc	% of total emulsion	atoms/cc$\times10^{22}$	(nucleons/cc)$\times10^{22}$
Ag	1.82	47.5	1.02	109.8
Br	1.34	35.0	1.01	80.6
N, O, C	0.60	15.7	2.65	36.2
H	0.053	1.39	3.17	3.19
others	0.015	0.39	0.02	1.14
Total	3.83	100.0	4.60 (excluding H)	230.93

average atomic weight of an emulsion nucleus). The number of equivalent quanta Q, in a bremsstrahlung beam, is the integrated energy of the beam W, divided by the peak energy E, i.e., $Q=W/E$. When normalized in this manner, the cross section per photon of energy k may be obtained by taking the slope of a plot of σ_Q vs $\ln E$; i.e., the photon cross section $\sigma_k=d\sigma_Q/d(\ln E)$. This is often called the "photon difference method," since it amounts to saying that the difference in yields between two bremsstrahlung energies E_1 and E_2 is due to photons having energies between E_1 and E_2.

The cross sections have been corrected for scan efficiencies and background. Table I includes the previously published data from I (3000 stars) as well as present measurements (7000 stars). The excellent agreement under different exposure conditions indicates the consistency of the monitoring and photostar counting measurements. The indicated errors, while primarily statistical, include estimates of the errors in background and scan efficiency, etc., as discussed in I.

The yields in Table I have been expressed in terms of the total number of nucleons in the target emulsion. The composition of Ilford G-5 emulsion is given in Table II. It will be shown that the probability for star formation after the occurrence of a mesonic event is roughly independent of nuclear size over a wide range of elements. Hydrogen cannot give a multiple-charged star as a result of a single pion process, but no attempt has been made to treat it separately, since it contributes only 1.5% of the total number of nucleons.

In order to compare our results with those of other workers we group all stars of 2-or-more prongs, and 3-or-more prongs and normalize per emulsion nucleus (excluding hydrogen). Figure 1 shows the data previously displayed in I, plus our new data and those of Castágnoli *et al.*[15] The yield ($49.6\sigma_Q$) is plotted vs $\ln E$, and the solid curve is a visual fit to our data. The principal difference in experimental technique between this work and that of Castagnoli *et al.* is in the scanning technique; they used a sampling method, normalized by photometric means. Both groups agree as to the yield of stars of 3 or more prongs at 1100 Mev, but they find lower values near 500 Mev and, therefore, a steeper slope. Their average slope yields a photon cross section of 306 ± 60 μb/nucleon in

[15] C. Castágnoli, M. Muchnik, G. Ghigo, and R. Rinzivillo, Nuovo cimento **16**, 683 (1960).

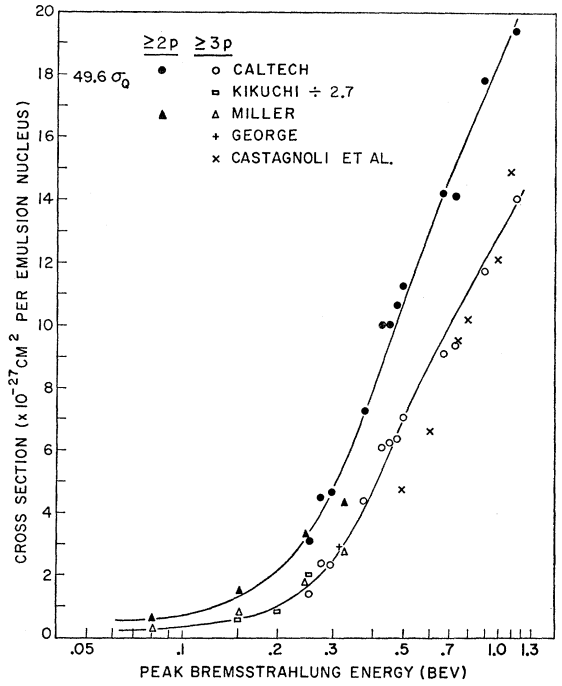

FIG. 1. The integrated cross section per Q per emulsion *nucleus* (excluding H) for photostars with two or more prongs, and three or more prongs, as a function of maximum bremsstrahlung energy. Points at lower energy include those of Miller, Kikuchi, and George (see I), and at higher energy those of Castagnoli *et al.* The solid lines are visual fit to our experimental points. A constant slope implies that the cross section per photon is constant.

the energy interval 500–1100 Mev, whereas our data give 240±50 μb/nucleon. The constant slope above 300 Mev implies a constant cross section per photon. The cross section is observed to be quite low at the mesonic threshold and then to rise quite steeply. The low photostar yield at 150 Mev includes all of the ≥2-prong events which might come from the "giant resonance" or the quasi-deuteron processes below the mesonic threshold. Miller has identified 20% of these nonmesonic ≥2-prong photostars as $C(\gamma,3\alpha)$ and $O(\gamma,4\alpha)$ events.

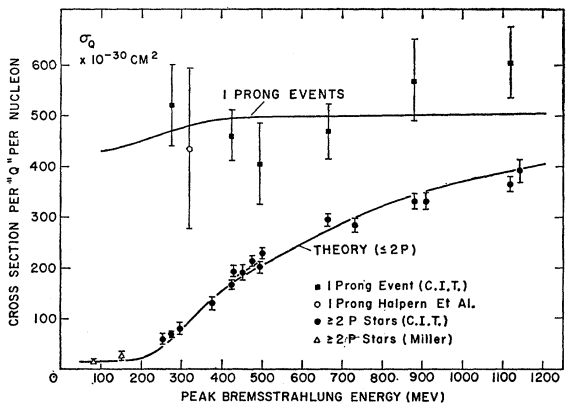

FIG. 2. The integrated cross section σ_Q per *nucleon* as a function of peak bremsstrahlung energy for photostars of two or more prongs, and for one-prong stars alone. Note that most of the one-prong photostars are contributed by low-energy photons. The large errors reflect the difficulty in measuring single-prong events. The solid line marked "theory" is the prediction of our model for multiprong stars (see "Interpretation of Results").

1-Prong Stars

The ratios of one-prong to ≥2-prong events were measured in several sample regions at a series of bremsstrahlung energies. Figure 2 shows these 1-prong yields as well as the ≥2-prong data. Figure 2 also includes the one point obtained from the radiochemical work of Halpern *et al.*[16] They bombarded Cu with 320-Mev bremsstrahlung and analyzed the resulting isotopes. Using their ratio of isotopes with $\Delta Z=1$ to those with $\Delta Z\geq 2$ and our ≥2-prong cross section the 1-prong cross section was determined. The rather good agreement between two very different methods is encouraging.

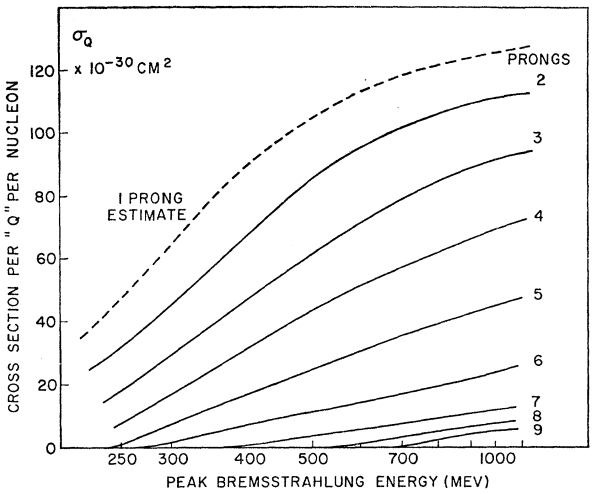

FIG. 3. Bremsstrahlung yield of photostars of various prong numbers, as indicated to the right of each curve, as a function of peak bremsstrahlung energy. This is a plot of the data of Table I.

The errors in our 1-prong points come primarily from the estimates of the amount of beam striking the sample area, determined by counting ≥2-prong stars. More than 90% of the 1-prong events have kinetic energies of less than 20 Mev. The high yield at the mesonic threshold strongly indicates that most 1-prong events are made by low-energy protons. This is consistent with the data from counter experiments.[5,7]

Excitation Curves for Various Prong-Number Stars

The measured excitation curves for stars with different prong numbers are shown as solid curves in Fig. 3. The relative greater importance of low-prong-number stars at the lower energies is rather marked. The slope of the curve for two-prong events flattens out after 800

[16] I. Halpern, R. J. Debs, J. T. Eisinger, A. W. Fairhall, and H. G. Richter, Phys. Rev. **97**, 1327 (1955).

Mev, indicating that the higher energy photons have reduced cross sections for the production of 2-prong stars. The second significant point is the "threshold" for each prong multiplicity. A minimum energy of 50 to 75 Mev/prong is required before the excitation function slopes upwards to a significant degree. The almost complete absence of ≥ 8-prong stars for bremsstrahlung of less than 500 Mev and their frequent production at higher energies can be seen in Table I. The highest prong number star (14 prongs) observed in this experiment was seen in a plate exposed at 1.15 Bev and is shown in Fig. 4. The visible energy of this star was 428 Mev. Since one would expect over half the energy to be carried away by neutrals, it is most likely this event was produced by a Bev photon.

There seem to be a few 1-prong events made by photons above the pion threshold, although it is difficult to measure accurately the high-energy component in the midst of so many low-energy events. We can only estimate a "reasonable" excitation curve for 1-prong events from high-energy photons, and then see if the integrated yield is roughly in agreement with the observations. We have drawn an "estimated 1-prong" dashed curve in Fig. 3 on the following basis: The shape is similar to the 2-prong curve, but the threshold for the 1-prong curve is lower. The resulting total 1-prong yield is then plotted in Fig. 2, and is not in disagreement with observed numbers of 1-prong events.

TABLE III. Stars observed in the 1143-Mev stack exposure, classified as to number and type of prong observed. Events with multiple pions and/or alphas are shown in parenthesis. Some stars had both pion and alpha prongs.

	Number of stars with ···				
Star prong number	≥ 1 stopping pions	≥ 1 fast prongs	≥ 1 alphas	Only protons	Total stars
2	0	2	1	29	31
3	3	1	2, (1)	13	19
4	4	0	2, (1)	13	20
5	3	0	4, (1)	12	19
6	1	1, (2)	3, (1)	7	13
7–9	1	0	1, (1)	5	8
10–13	1	0	2, (1)	2	5
Totals	13	6	15, (6)	81	115

Characteristics of 1150-Mev photostars.—The visible energy release, prong angular distributions, etc., for $130 \geq$ 2-prong photostars produced by 1150-Mev bremsstrahlung were measured with an emulsion pellicle stack exposure. The pre-exposure background was eliminated by examining only stars whose prongs could be traced through the stack. All star prongs were traced and their range and ionization were measured. This will discriminate against these low-energy stars whose prongs all end within the same pellicle. The identity of each prong was determined by ionization and range measurements.

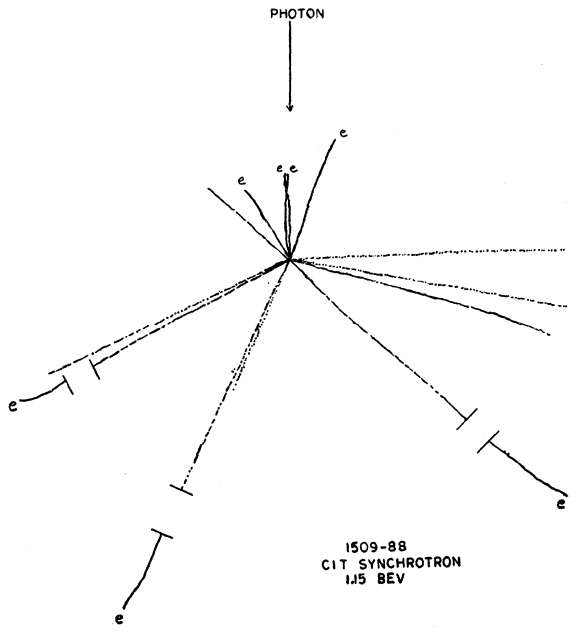

FIG. 4. Fourteen-prong photostar produced by 1.15-Bev bremsstrahlung. The visible energy release was 428 Mev.

There was no attempt made to separate protons from deuterons; however, the alphas and low-energy pions were reliably identified. A 3-prong star formed by a 25-Mev π^- photostar prong is shown in Fig. 5. The stars have been classified according to prong type and prong number in Table III. Most of the prongs are protons; 75% of the stars do not emit any other type of particle. Stars with one or more pion prongs which stop or lose most of their energy in the emulsions are listed separately from those with fast prongs which escape. These fast prongs could be either pions (≥ 30 Mev) or fast protons (>200 Mev). If these fast prongs are all classified as pions, then 16% of the ≥ 2-prong stars have one or more pion prongs.

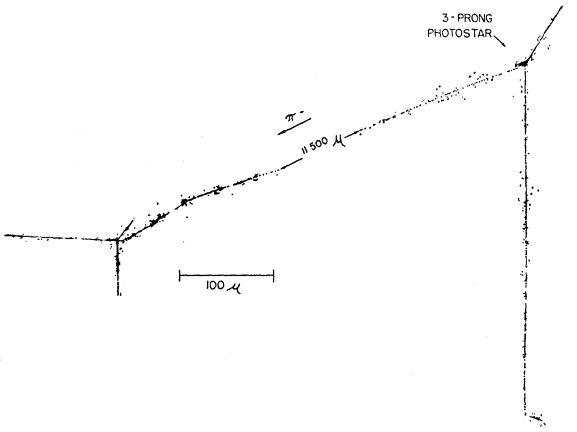

FIG. 5. Double star resulting from 25-Mev π^- photostar prong. Several such mesonic events were observed.

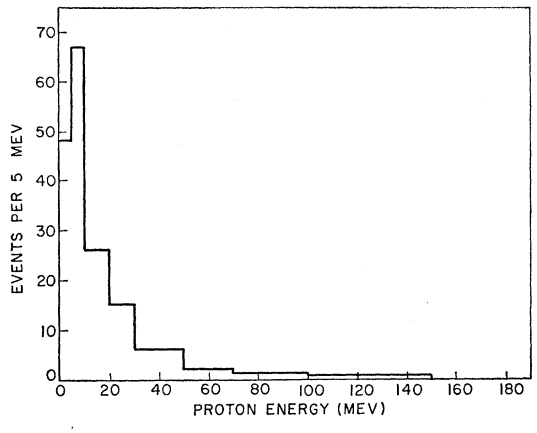

FIG. 6. Energy spectrum of star prongs (protons only) produced by 1150-Mev bremsstrahlung. Most of the proton energies were determined by range measurement; the higher energies were often based on gap counting.

The energy distribution of the proton prongs is shown in Fig. 6. The abundance of the low-energy 10–30 Mev prongs would be expected by nuclear evaporation processes. The high-energy protons are most likely nuclear cascade particles. The drop-off below 5 Mev is due to scanning bias and Coulomb effects. Some 20% of the observed proton prongs had energies below 5 Mev, well below the Coulomb barrier for the heavy elements (Ag and Br). This is in agreement with the results reported earlier in I: the low-energy protons are quite common and are presumably emitted by the heavier elements in spite of the Coulomb barrier. (See Sec. IV).

The visible energy release per star, including the binding energy of each prong, is shown in Fig. 7. The average visible energy associated with each prong number is shown in Fig. 8. Stars with larger prong numbers have been grouped because of the limited statistics. The "average" photon energy associated with each prong number has been obtained from Fig. 3 by taking the photon energy at half-height on the excitation curve. Both the mean visible energy and the mean photon energy increase approximately linearly with prong multiplicity.

The angular distribution of the proton prongs is shown in Fig. 9. The angles shown are space angles referred to the direction of the incident photons. The prongs have been divided into 3 energy ranges which roughly agree with the phenomenological classification of black, gray and light used in the excitation measurements. The forward/back ratios given in Table I can be compared with the values from the detailed measurements. The forward peaking with increasing prong energy is quite noticeable.

The transverse momentum unbalance which gives a lower limit for the energy carried off by neutrals, and the longitudinal momentum which also gives a measure of the incident photon energy, were measured. No particular pattern was observed. The data are consistent with the assumption that more than half the star's energy is carried off by neutrals.

Unusual Events.—A triple star was found in an emulsion exposed to 665-Mev bremsstrahlung. The primary star and the two secondary stars (presumably from π^- mesons) are seen in Fig. 10. The 1.2-μ separation is so short that one cannot identify the particle. The star density is such that the probability of a chance coincidence of two stars is much less than 10^{-6}. The event can

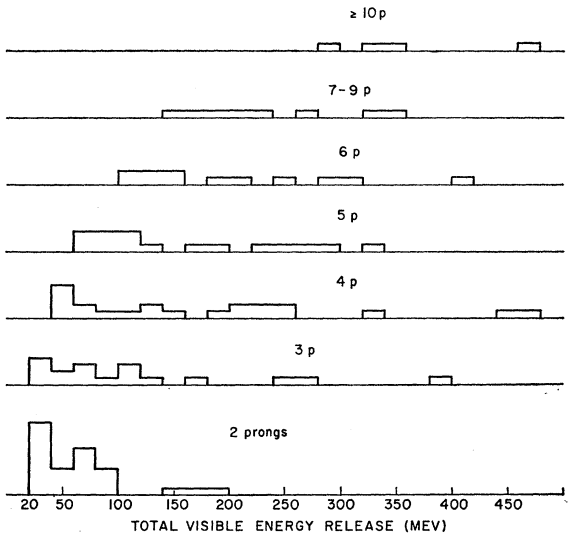

FIG. 7. Total visible energy release per star for photostars of various prong numbers. Total energy includes all binding energies, and the mass energy of any pion which might be emitted.

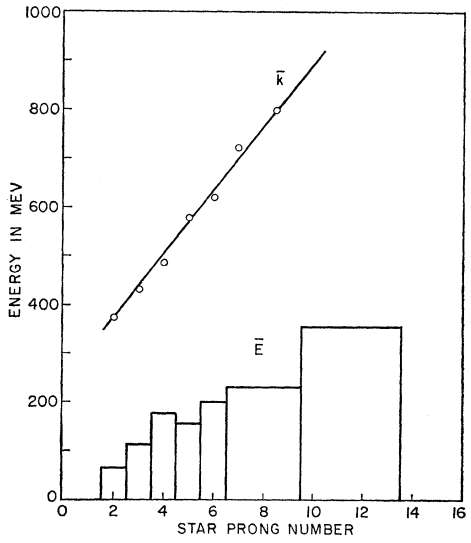

FIG. 8. Average visible excitation energy including particle binding energies (E) observed for stars of various prong numbers. Also shown is the mean energy (k) of the photons producing the stars, taken as the photon energy at half-maximum in Fig. 3.

be understood as $\gamma+n\rightarrow\pi^{+}+2\pi^{-}+p$ with both π^{-} mesons escaping from the primary nucleus and forming secondary stars. There was no systematic attempt to follow star prongs in the single emulsion exposures, but several dozen slow pions were observed to form secondary stars (see Fig. 5).

In Fig. 11 a deuteron is observed to be emitted in the *backward* hemisphere and to cause the breakup of N^{14} in the reaction $H^{2}+N^{14}\rightarrow O^{16*}\rightarrow 4\alpha$. This is one of two such events with backward deuteron emission which was observed. The "quasi-deuteron" model would predict the occasional ejection of a deuteron in the forward direction, but the backward emission in the laboratory system implies the deuteron remains intact after a hard scattering within the nucleus.

IV. INTERPRETATION OF RESULTS

For the reasons presented in I and summarized in the Introduction to this paper, the most plausible model for high-energy photodissociation is the photoproduction and reabsorption of real pions within the nucleus. Previous results on the energy dependence of the photostar yield were shown in I to be consistent with this model. The present data reinforce this view, with better statistics and over a much broader range of gamma-ray energies.

Energy Dependence of Photostar Yield

With the real pion model the photostar yield is closely related to the total photomeson production cross section. Using experimental free-nucleon photomeson cross sections and the optical model of the nucleus, one can calculate the probability that photopions produced uniformly throughout the nucleus will be reabsorbed in the same nucleus, resulting in a photostar. Nuclear motion may be taken into account by calculating a photon energy resolution function. The recoil nucleon in the photoproduction process will often produce a nucleon cascade within the nucleus. The resulting "predicted curve" fits the photostar excitation date very closely.

The experimental cross sections for photomeson production and photodisintegration of the deuteron are taken from the published data of various groups at the

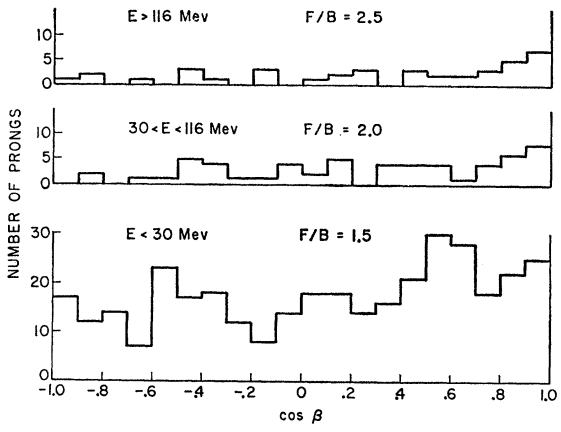

FIG. 9. Space angle distribution of proton prongs from photostars produced by 1150-Mev bremsstrahlung. The angle β is the space angle between the incident gamma ray and emerging proton. The data are grouped according to E, the kinetic energy of the proton. The forward-to-back ratios (F/B) are indicated, and increase with increasing proton energy.

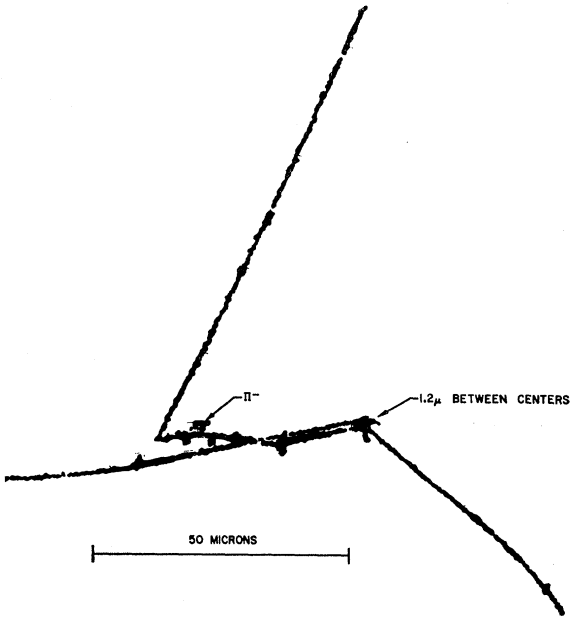

FIG. 10. Triple star produced by 665-Mev bremsstrahlung. The event can be understood as an example of triple meson production $\gamma+n\rightarrow\pi^{+}+2\pi^{-}+p$ with both π^{-} forming secondary stars, or it can result from a combination of $\gamma+n\rightarrow\pi^{-}+\pi^{0}+p$ with a subsequent charge exchange scatter of the π^{0}. ($\pi^{0}+n\rightarrow\pi^{-}+p$).

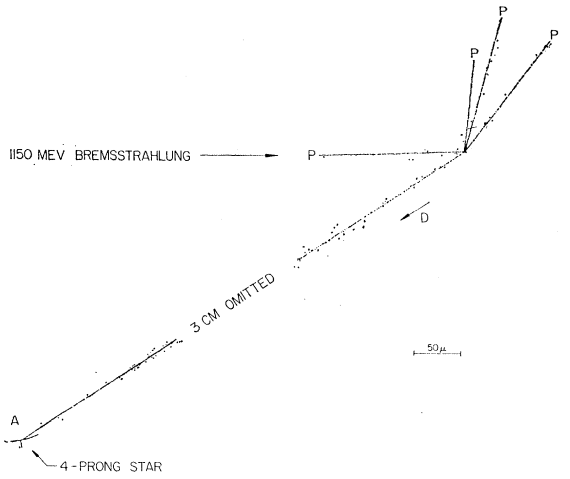

FIG. 11. A deuteron is emitted in the backward hemisphere. Its energy at the secondary star was very carefully measured and is consistent with the reaction $H^{2}+N^{14}\rightarrow O^{16*}\rightarrow 4\alpha$. Kinematically the deuteron could not be ejected in the backward hemisphere as a result of a single interaction.

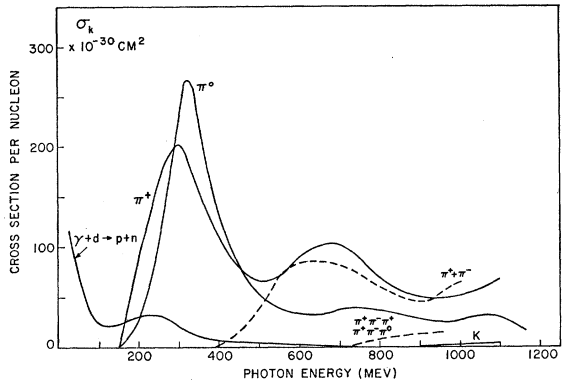

FIG. 12. Summary of known total cross sections for single and multiple photomeson production from free protons, elastic photodisintegration of the free deuteron ($\gamma+d\rightarrow p+n$), and photo-K-meson production ($\gamma+p\rightarrow K^+ +\Lambda^0$) as a function of photon energy. The photon cross sections are per nucleon.

CalTech and Cornell electron synchrotrons.[17] More recent data from the Frascati (Italy) electron synchrotron are generally in agreement with the earlier results, at least to the accuracy required here. The energy dependence of the total cross section is shown in Fig. 12, where the values are given *per nucleon* (the deuteron cross section is divided by two). In constructing the pion-pair contribution we have included neutral as well as charged pions, assuming equal cross sections for each possible reaction. The K-meson and triple-pion yields are small, but have been included for completeness. Note that the elastic photodisintegration of the deuteron is relatively improbable compared with processes producing real pions at energies above 150 Mev.

In obtaining a total yield for each nucleus, we have made several corrections to mere multiplication by the number of nucleons A. First of all, we have enhanced the deuteron photodissociation cross section by a factor of $6.4NZ/A=1.6A$ as proposed by Levinger[3] to take account of the Pauli principle. Secondly, we have considered the possible enhancement of pion yields as revealed from charged[18] and neutral[19] pion yield ratios from hydrogen and deuterium. It appears that the slight net increase in charged pion production is offset by a 10% decrease in neutral pions from the neutron. The total photopion cross section from the neutron is very close to the total photopion cross section from the proton.

The resulting total cross sections, for photopion production from a nucleon and for photodisintegration of a "pseudo-deuteron" (divided by 2), are shown in Fig. 13. These cross sections are expressed *per nucleon* by summing all the yields in Fig. 12 with the appropriate weighting factors. For example, we have multiplied the measured cross section for $\gamma+p\rightarrow p+\pi^+ +\pi^-$ by 3 to account for the expected yield of $(p\pi^0\pi^0)$ and $(n\pi^+\pi^0)$ products. The triple pion cross section is multiplied by $\frac{3}{2}$. As a result the second resonance is as high and more broad than the first resonance at 300 Mev. The majority of the cross sections are known experimentally only up to about 1 Bev, so that it is necessary to make some assumption as to the energy dependence of the sum of the cross sections up to about 1400 Mev for our model. This is because the Fermi momentum of the nucleons within complex nuclei can transform an 1150-Mev laboratory photon up (or down) 220 Mev in the rest system of the nucleon. We have chosen to assume an energy dependence indicated by the long-dashed line in Fig. 13 which is partially justified by evidence of a third resonance in both pion-nucleon scattering and photoproduction.

The short-dashed line in Fig. 13 shows the effect of nuclear motion in "smoothing out" the effective cross section energy dependence. This effective cross section for a given laboratory photon energy is obtained by averaging over the spread in "effective" photon energies allowed by the Fermi motion of the nucleon. Detailed calculations at three widely separated laboratory photon energies showed that the net effect was equivalent to a Gaussian spread of full width 30% of the mean photon energy, roughly independent of mean energy from 200 to 1100 Mev. Our final curve was then derived by weighting

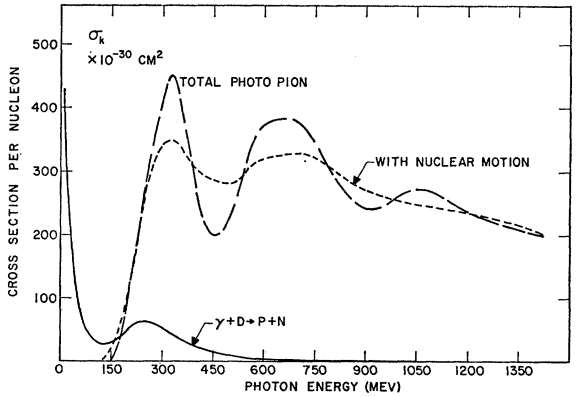

FIG. 13. Summation of all known high-energy photoprocesses (as given in Fig. 12) as a function of photon energy. The photomesonic cross sections assume no effects due to nuclear binding. The deuteron photodisintegration probability is enhanced by Levinger's factor ($6.4NZ/A$), but still remains small above 300 Mev. The effects of nuclear motion are estimated by the short-dashed curve; this is the curve used to construct the bremsstrahlung integral yield curve in Fig. 2.

[17] For π^+ cross sections see F. Dixon and R. L. Walker, Phys. Rev. Letters **1**, 1504 (1958). The π^0 cross sections are from K. Berkelman and J. Waggoner, Phys. Rev. **117**, 1364 (1960). The charged multiple-pion cross sections are given by B. Chasan, G. Cocconi, V. Cocconi, R. Schectman, and D. White, Phys. Rev. **119**, 811 (1960). The photodissociation of the deuteron has been measured up to 900 Mev by H. Myers, R. Gomez, D. Guinier, and A. V. Tollestrup, Phys. Rev. **121**, 130 (1961). See these papers for references to earlier work, particularly at lower energies.

[18] G. Neugebauer, W. Wales, and R. L. Walker, Phys. Rev. **119**, 1726 (1960).

[19] H. H. Bingham, Ph.D. thesis California Institute of Technology, Pasadena, California, 1959 (unpublished). J. C. Keck, A. V. Tollestrup, and H. H. Bingham, Phys. Rev. **103**, 1549 (1956).

the mean energy twice, and points at ±15% energy shift at single weight. It is clear from Fig. 13 that nuclear motion washes out detailed structure, although it also has the effect of extending the peak energy past the nominal limits of the bremsstrahlung.

We have assumed all nucleons to be equally probable sources of photopions, since high-energy photons have long mean-free-paths for interaction in nuclear matter. Thus our model visualizes real pions emerging from random points within the nucleus, a situation quite different from pions produced within complex nuclei by strongly interacting particles. In order to make a multiprong photostar, we then assume that at least one of the following must occur: (a) scattering or absorption of a single pion exciting the nucleus, so that at least two charged particles escape, (b) scattering of a fast recoil nucleon, giving rise to at least one additional charged particle besides either a charged meson or recoil proton, or (c) multiple charged-pion photoproduction with or without subsequent interaction. Insofar as these secondary processes are highly probable, photostar production is a measure of the total photoproduction of strongly interacting particles. If we define this over-all "absorption probability" as P_a, then for a nucleus of A nucleons the photostar cross section will be

$$\sigma_{\text{star}}=\sigma_f A P_a,$$

where σ_f is the free-nucleon cross section of Fig. 13, with nuclear motion taken into account.

The simplest calculation of P_a would be to use the optical model and assign a mean free path in nuclear matter, λ, to the pions. This has been done by Francis and Watson[20] to explain the $A^{\frac{2}{3}}$ dependence of photomeson yields, and by Reff[21] to try to account for the early photostar data. The result for photostars is $P_a=1-3\lambda/4R$, where R is the nuclear radius, and only absorption of pions is assumed. If we add the independent probability that the recoil *nucleon* can produce a star by assigning a nucleon mean free path λ_n as well as a pion mean free path λ_π then $P_a=1-9\lambda_\pi\lambda_n/16R^2$. Following the optical-model prescription of Frank, Gammel, and Watson[22] for computing mean-free paths, we find $P_a\simeq 0.9$ for pion energies near and above the first resonance. This high and nearly constant probability is due to the combined star-producing effects of both pion and nucleon.

However, we have *not* adopted the above optical model formulation in so simple a form because of the availability of much more refined Monte Carlo calculations of Metropolis *et al.*[23] on pion- and nucleon-initiated cascades which take account of many effects not included above. For example, the Monte Carlo calculations include the effect of the Pauli principle and of Coulomb barriers. The numbers and types of cascade particles, and excitation of the residual nucleus are given as function of incident energy. Metropolis *et al.* also give the transparency of a nucleus (such as Ru^{100}, similar to AgBr) for pions and protons of various incident energies. We have made one important change in the numbers of Metropolis *et al.*: We have doubled their transparencies, because our photopions and nucleons originate uniformly within the nucleus, rather than impinge from the outside, and hence have only ½ the average path-length. If T_π and T_n are pion and nucleon transparencies, then the star production probabilities are $P_\pi=1-T_\pi$ and $P_n=1-T_n$. The combined star probability is then $P_a=P_\pi+P_n-P_\pi P_n$. Table IV lists the star production probabilities for the most probable (90° c.m.) pion and recoil nucleon produced by various energy photons, and gives the resulting star probability P_a. At low photon energies P_a is quite low, since the pion has a long interaction distance and the recoil nucleon has insufficient energy to produce a cascade. After the first resonance P_a is nearly constant at 0.8. The recoil nucleons are as important as the pions at photon energies above 700 Mev.

TABLE IV. Probability for star formation in the Ru^{100} nucleus by photoproduced pion or recoil nucleon in $\gamma+N\rightarrow\pi+N$. P_π and P_n are star production probabilities, and $P_a=P_\pi+P_n-P_\pi P_n$.

Photon energy (Mev)	Mean pion kinetic energy (Mev)	P_π pion probab.	Mean nucleon kinetic energy (Mev)	P_n nucleon probab.	P_a star probability
175	18	0.15	15	0	0.15
200	37	0.33	20	0	0.33
250	73	0.50	35	0.14	0.57
300	107	0.75	50	0.20	0.80
400	180	0.80	80	0.30	0.86
500	245	0.72	115	0.34	0.81
700	379	0.58	182	0.55	0.81
900	495	0.53	265	0.65	0.83
1100	630	0.58	330	0.65	0.85

It is now possible to construct a photostar excitation curve on the basis of our model, which has no free parameters. Using values of P_a from Table IV, we integrate $\sigma_k=\sigma_{\text{star}}/A$ over the bremsstrahlung spectrum to arrive at the solid curve marked "theory" in Fig. 2. The comparison is with stars of 2 or more prongs, since in computing P_a we have included the probability that either the pion or proton produce at least one charged particle. Furthermore, Metropolis *et al.*,[23] show that the nucleus is left excited so that at least one or more additional charged particles will be evaporated. The agreement between theory and experiment is quite satisfactory, although the predicted yield of stars is lower than the observed yield at energies just above the mesonic threshold. This is undoubtedly due to the fact that we have not included the multiprong stars made by cascades from the "pseudo-deuteron" photodisintegra-

[20] N. C. Francis and K. M. Watson, Phys. Rev. **89**, 328 (1953).
[21] Israel Reff, Phys. Rev. **91**, 150 (1953).
[22] R. M. Frank, J. L. Gammel, and K. M. Watson, Phys. Rev. **101**, 891 (1956).
[23] N. Metropolis, R. Bivins, M. Storm, A. Turkevich, J. M. Miller, and G. Friedlander, Phys. Rev. **110**, 185 (1958).

tions in our calculations. It is just in this range that the fast nucleons from the process $\gamma+d \rightarrow p+n$ would often have enough kinetic energy to initiate cascades. Furthermore, it is only in this interval that the cross section for deuteron photodisintegration is comparable with the photopion cross section.

We conclude that both the magnitude and shape of the photostar bremsstrahlung yield σ_Q is well understood on the basis of our model, without the need of adjustable parameters.

It is of interest to note that the intimate connection between photopion production from free nucleons and photostars from complex nuclei, together with the effects of nuclear motion in extending the energy interval involved, allow limited "predictions" of the approximate total photopion cross section at higher energies. As noted in I, the continued steep rise of the photostar yield at 500 Mev, despite a rapid drop in the single-pion photoproduction cross section, was an indicator of the (then unknown) second resonance and large multiple pion yields. The constant slope of the σ_Q vs $\ln E$ plot near 1100 Mev indicates that the sum of photopion processes continue to have approximately the same photon cross section out to 1400 Mev.

A few remarks can be made about the 1-prong star yield, also shown in Fig. 2. Most of the single-prong events are low-energy protons due to photons below 150 Mev. The magnitude of the yield at 150 Mev is in reasonable agreement with the assumption that the 1-prong stars are due to (γ,p) reactions of the giant resonance plus pseudo-deuteron disintegrations with the enhanced cross section shown in Fig. 13. The additional rise in 1-prong events above 150 Mev cannot be due only to the dwindling deuteron dissociation. Some of the single prongs are pions which escape from the nucleus without interacting, either in conjunction with a non-interacting recoil neutron or a low-momentum recoil proton which cannot escape the nucleus. Rare cases of stopping pions which "start" in the emulsion are seen. However, a thorough study of the pion fraction of prongs, especially in 1-prong stars, has not been made. Our model would suggest that 1-prong stars should constitute a smaller fraction of all photostars as the photon energy increases. This results in the dashed curve in Fig. 3, which is essentially an informed guess as to how meson-induced single-prong events might occur. When the low-energy yield is added, the solid curve of Fig. 2 for 1-prong events results.

Prong Numbers of Photon-, Proton-, and Pion-Induced Stars

In this section we discuss the variation of the prong number with the energy available to make the star, and show similarities between stars initiated by gamma rays, protons, and pions. We also attempt to determine the average excitation of the residual nucleus, after the initial cascade, by observing how many "evaporation" prongs occur.

We define "available energy" as the kinetic energy of the incident particle, plus its rest mass if it can be absorbed. Thus 140 Mev is added to the kinetic energy of the pion. We compare our photostars with the stars in nuclear emulsion produced by protons of 140 Mev,[24] 350–400 Mev,[25] and 950 Mev,[26] and by pions of 70–90 Mev,[27] 162 Mev,[28] and 500 Mev.[29]

Since *photon* (not peak bremsstrahlung) energy is our independent variable in this analysis, we must differentiate σ_Q in Fig. 3 in order to obtain the photon cross section σ_k for each prong number. The dashed curve is used for 1-prong stars; i.e., only high-energy 1-prong stars are included. The fraction of 0-prong stars among photostars was taken to be 5%, which is an average figure for pion- and proton-induced stars in the same energy range.

In Fig. 14 we have plotted *mean* prong number vs available energy for emulsion stars initiated by photons, protons and pions. The mean prong number is essentially independent of the nature of bombarding particle, and is a function only of the available energy. One can interpret this result as a lack of sensitivity of mean prong number to different possible models of photodisintegration, or alternatively as additional evidence that high-energy photostars are produced by cascading pions and nucleons within the nucleus.

Metropolis *et al.*[23] calculate the average number of charged cascade particles emitted for various values of pion or proton kinetic energy, and we have summarized their results by the line marked "Cascade" in Fig. 14. The observed mean prong number is about 2 prongs above the cascade line for all energies. Dostrovsky *et al.*[30] in their Monte Carlo evaporation calculations, show that one can expect on the average two charged particles for each 100 Mev of excitation energy of a heavy nucleus. We thus conclude that the cascade process leaves the residual nucleus with about 100 Mev excitation energy, over a wide range of incident bombarding energies.

The energy distribution of photostar prongs has been studied carefully at only one bremsstrahlung energy (1143 Mev, see Fig. 6), so that we do not have data on the *photon* energy dependence of the number of "black" prongs per star. However, the integrated data at 1143 Mev are consistent with 2 evaporation protons per star plus additional cascade protons. Lees *et al.*[24] have shown

[24] C. F. Lees, G. C. Morrison, H. Muirhead, and W. G. V. Rosser, Phil. Mag. **44**, 304 (1953).
[25] G. Bernardini, E. T. Booth, and S. J. Lindenbaum, Phys. Rev. **85**, 826 (1952).
[26] W. O. Lock, P. V. March, and R. McKeague, Proc. Roy. Soc. (London) **A231**, 215 (1955).
[27] G. Bernardini, E. T. Booth, S. J. Lindenbaum, and J. Tinlot, Phys. Rev. **82**, 105 (1951).
[28] R. A. Nikol'skii, L. P. Kudrin, and S. A. Ali-Zade, Soviet Phys.—J.E.T.P. **5**, 93 (1957).
[29] M. Blau and M. Caulton, Phys. Rev. **96**, 150 (1954).
[30] J. Dostrovsky, P. Rabinowitz, and R. Bivins, Phys. Rev. **111**, 1659 (1958).

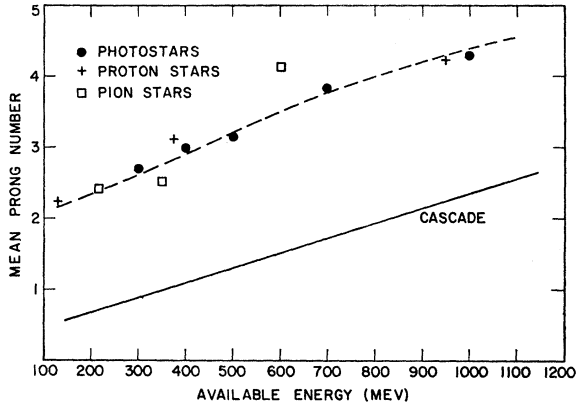

FIG. 14. Mean prong number for photostars, pion-, and proton-induced stars in nuclear emulsion as a function of "available energy." "Available energy" is the laboratory kinetic energy of the bombarding particle plus rest mass energy in case of the pion. The curve marked "cascade" is our summary of the Monte Carlo calculations of pion- and proton-initiated nuclear cascades by Metropolis *et al.*[23] The additional prongs are presumably due to evaporation from the excited residual nucleus.

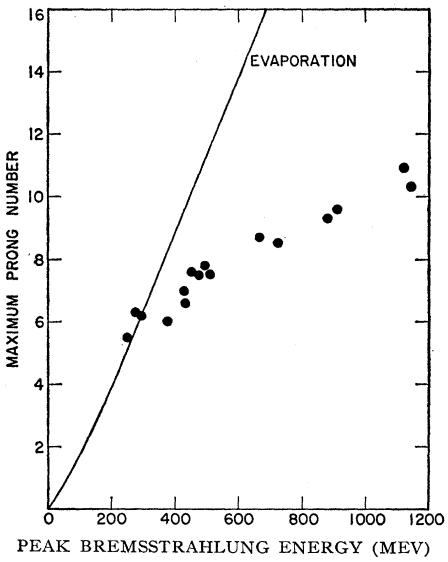

FIG. 15. Maximum prong number of photostars as a function of peak bremsstrahlung energy. The maximum prong number is the average prong number of the largest 2% of the stars. The solid line represents the maximum prong number expected if the maximum energy photon gave all its energy to nuclear excitation. This becomes more improbable as the energy increases.

from the angular distribution of low-energy proton prongs observed in proton-induced stars that some protons are "low-energy debris" of nuclear cascades.

Infrequently one might expect the excitation energy of the nucleus to be a large fraction of the available energy, in which case most of the prongs would be evaporation prongs and the maximum prong number would occur. In Fig. 15 we have plotted the "maximum prong number" of the photostars for each exposure against peak bremsstrahlung energy. The "maximum prong number" is defined as the average prong number of the top 2% of the stars. The solid curve is the predicted number of prongs if peak gamma-ray energy went entirely into excitation. It is to be noted that only for lower energies is the agreement at all satisfactory, and at higher energies the maximum prong number falls well below this maximum. We interpret this as a demonstration that it is extremely difficult to excite the nucleus as a whole more than 100 Mev or so, but that most of the energy is carried away by the cascade.

The Monte Carlo calculations also predict that more than half of the incident energy will be carried away by neutral prongs. As noted earlier in Fig. 8, the average visible excitation energy for a given prong number is less than half of the mean energy of the photon producing the star.

Stars from Light and Heavy Nuclei

It is reasonable to believe that at very high energies the initial elementary interactions will be with nucleons. We have also demonstrated that the absorption process is not strongly dependent upon nuclear size due to the combined probability of interaction by pion or recoil nucleon. Hence, we have assumed that the photostar cross section is very nearly proportional to A, the mass of the nucleus.

Earlier treatments of photostar production, however, have noted the existence of slow protons amongst the prongs of the multiprong stars, and have attributed them to light elements wherever the kinetic energy of the prong was below the Coulomb barrier for the stable isotopes of Ag or Br. For example, Miller[8] concluded that 45% of his photostars ($\leq$3-prong) at 330 Mev were from C, N, or O, even though these light elements constitute only 16% by weight of nuclear emulsion. The prong range cutoff was 50 μ (2.3-Mev proton).

We noted in I that similar results occurred in our 500-Mev bremsstrahlung photostars, namely, 47% of the $\geq$3-prong stars had at least one prong shorter than 50 μ. However, an alternative explanation was presented: namely, that the low-energy protons were merely the natural aftermath of the nuclear cascade which leaves the residual nucleus "proton-rich" and energetically more likely to decay by proton emission than by neutron or gamma emission despite the Coulomb barrier. This postulate was supported by nuclear chemical evidence of Debs *et al.*[31]

The Monte Carlo calculations of Metropolis *et al.*[23] now give added support to this idea of preferred proton emission. Neutrons have longer mean-free paths than protons because of the difference in the *n-p* and the *n-n*, *p-p* scattering cross sections. Furthermore, the neutron's Fermi energy is a larger fraction of the energy required for a significant cascade process.

Lees *et al.*[24] in a study of stars induced by 140-Mev protons, noted that the forward-back ratio of their low-

[31] R. J. Debs, J. T. Eisinger, A. U. Fairhall, I. Halpern, and H. G. Richter, Phys. Rev. **97**, 1325 (1955).

energy protons indicated that a substantial fraction were not evaporation protons, but low-energy "debris" from nuclear cascades.

Another objection to ascribing many photostars to light elements on the basis of Coulomb barrier arguments is that it seems quite improbable that any light element excited by high-energy photons could stay together as a nucleus long enough to evaporate a low-energy proton.

Hence, we neither use the short prongs for a light-heavy separation, nor do we consider their existence as evidence against our model for photostars.

V. COMPARISON WITH THE "SUPPRESSED CORE" MODEL

Butler[32] some time ago proposed a model in which photopion production is "suppressed" in the central portion (or "core") of the nucleus, in order to explain the $A^{\frac{2}{3}}$ dependence of the photomeson yield from complex nuclei. Estimates of the absorption mean free path for pions in nuclear matter were in the range of 8 fermis, due to the low kinetic energies of the existing experiments. Subsequently Francis and Watson[20] showed that the optical model was quite sufficient to explain the observed photomeson yields, using the same mean-free-path values, if the effects of nuclear binding were considered.

Our present data and calculations agree with the view that the optical model is sufficient to explain not only photomeson production, but also the production of photostars. Much more complete data on pion and nucleon interaction lengths are now available, and the Monte Carlo calculations establish firm predictions for nuclear cascades. It seems clear that there is no need for any core suppression, but rather that it is easy to see why relatively few pions escape from the center of a heavy nucleus on the basis of short mean free paths.

[32] S. T. Butler, Phys. Rev. **87**, 1117 (1952).

Belousov *et al.*[33] have found that the $A^{\frac{2}{3}}$ dependence of the photopion yield holds for low-energy (20 Mev) as well as for higher energy (65 Mev) neutral pions. Since the mean free path for absorption of pions within nuclear matter varies considerably over this energy interval, they have interpreted their results as evidence for surface *production* of pions. This is similar to Butler's suppression of pion production in the core. One must consider the actual values of the mean free paths, relative to the nuclear radius, in assessing the sensitivity of this test. The optical model values[20] are sufficiently short [$\lambda_\pi \approx 10(\mu/\hbar c)$ for 20-Mev pions inside nuclear matter] that the reabsorption is significant even for low-energy pions in light nuclei. For reasonably short mean free paths an $A^{\frac{2}{3}}$ dependence is expected on either the suppressed core model or optical model.

ACKNOWLEDGMENTS

One of us (C.E.R.) wishes to thank the Research Corporation for its support of that part of the program carried out at the University of California at Riverside. Mr. George Van Buskirk, Mr. Kenneth Crowder, Miss Jean Coulson, and Mr. William Baskett were of great assistance in scanning the excitation function plates. The exposures were made at California Institute of Technology's 1.2-Bev electron synchrotron, as part of a program of high energy nuclear physics research supported by the U. S. Atomic Energy Commission. The support and encouragement of Dr. R. F. Bacher is gratefully acknowledged. We have had several illuminating conversations with Dr. R. F. Christy concerning points of theory. Additional scanning, cross checks, and the 1150-Mev stack investigation were done by the CalTech scanning team of Mrs. Elaine Motta, Mrs. Nancy Gross, Mrs. Judith Lundalius, Mrs. Laura Patterson, and Mrs. Cheryl Maloy.

[33] A. Belousov, V. Popova, N. Semashko, E. Shitov, E. Tamm, V. Veksler, and F. Iagudina, *Proceedings of the CERN Symposium on High-Energy Accelerators and Pion Physics, Geneva, 1956* (European Organization of Nuclear Research, Geneva, 1956), Vol. 2, p. 288.